Catena 174 (2019) 227–234

Contents lists available at ScienceDirect

Catena

journal homepage: www.elsevier.com/locate/catena

Mitigation of soil acidification through changes in soil mineralogy due to long-term fertilization in southern China

Liang Tao[a], Fang-bai Li[a,*], Cheng-shuai Liu[b], Xiong-han Feng[c], Li-li Gu[c], Bo-ren Wang[d], Shi-lin Wen[d], Ming-gang Xu[d]

[a] Guangdong Key Laboratory of Integrated Agro-environmental Pollution Control and Management, Guangdong Institute of Eco-environmental Science & Technology, Guangzhou 510650, PR China
[b] State Key Laboratory of Environmental Geochemistry, Institute of Geochemistry, Chinese Academy of Sciences, Guiyang 550081, PR China
[c] Key Laboratory of Arable Land Conservation (Middle and Lower Reaches of Yangtze River), Ministry of Agriculture, College of Resources and Environment, Huazhong Agricultural University, Wuhan 430070, PR China
[d] National Engineering Laboratory for Improving Quality of Arable Land, Institute of Agricultural Resources and Regional Planning, Chinese Academy of Agricultural Sciences, Beijing 100081, PR China

ARTICLE INFO

Keywords:
Soil acidification
Potential acid Al^{3+}
Al substituted iron oxides
Differential X-ray diffraction spectra

ABSTRACT

Soil acidification is a natural process, and it is well known that soil acidification can be accelerated by long-term fertilization (LTF). Nevertheless, how this acidification occurs and how the mineralogies of iron oxides as the important active clay components in red soil respond to the acidification is still less understood. In this study, soil samples from 23 years (1990–2013) of long-term fertilization experiments were collected from the Qiyang Red Soil Experimental Station in southern China. The physicochemical properties of the soil samples were analyzed. A significant negative linear correlation between soil pH and log(Al_{py}) (complex-state aluminum) as well as log(Al_{exch}) (exchangeable Al^{3+}) illustrate that Al_{py} and Al_{exch} are the most sensitive species to soil acidification compared with the other factors. In addition, the mineralogical characteristics of the iron oxides in five typical LTF treatments, including the control, chemical fertilizer N, NPK, NPK plus manure and manure were analyzed using the synchrotron differential XRD patterns (DXRD). The results obtained revealed that the LTF treatment with chemical N reduced the total content of iron oxides and the ratio of goethite to hematite (G/H value), and the transformation of iron oxides and accumulation of hematite in the soil would reduce the soil's buffering capacities to acidification. In contrast, the LTF treatments with manure (NPKM and M) presented the opposite trends. In addition, a positive relationship between soil pH and the $IOs_{Almol\%}$ (isomorphous substitution ratio of Al for Fe in iron oxides) was also found. Therefore, the potential acid Al^{3+} ions in soil are reduced through the ionic substitution of Al for Fe in the structure, which may further mitigate the process of soil acidification. These results provide new insights for further understanding the soil acidification processes induced by LTF and how those iron oxides respond to soil pH during soil acidification.

1. Introduction

Naturally acidic soil, which accounts for approximately 30% of the world's ice-free land (comprising up to 50% of the world's potential arable land), is commonly associated with a deficiency of one or more essential plant nutrients, Al toxicity, and reduced biodiversity and productivity (Blake et al., 1994; Bolan et al., 2003; Bünemann et al., 2018; Rice and Herman, 2012). Numerous studies have focused on the disruption of soil acidification on agricultural production, soil organisms and Al toxicity, which have proved that soil acidification has an adverse impact on both plants and soil organisms (Breemen, 1991; Speir et al., 1999). In China, red soil occupies an area of 1.13 million km^2, and approximately 6.5% (~57 Mha) of the total arable land is highly weathered acidic red soil (Ferralic Cambisol).

Soils generally acidify very slowly under natural conditions over hundreds to millions of years, but this can be accelerated by certain human activities. Under managed farming systems, most of the acidity is generated from the application of fertilizer and the biogeochemical cycles of C, N and S in soils. In the case of the C cycle, the two main sources of H^+ ions are (1) the dissolution of CO_2 to form H_2CO_3 in the soil solution and (2) the synthesis and dissociation of carboxylic acids produced by plants and microorganisms. The assimilation of CO_2 into

* Corresponding author.
E-mail address: cefbli@soil.gd.cn (F.-b. Li).

https://doi.org/10.1016/j.catena.2018.11.023
Received 10 April 2018; Received in revised form 9 November 2018; Accepted 16 November 2018
Available online 21 November 2018
0341-8162/

carboxylic acids produces H^+ ions, further acidifying the soil indirectly (Bolan et al., 2003). In the case of the N and S cycles, the mineralization and oxidation of organic N and S result in the production of H^+ ions, reflected in a decrease in pH in soils with a low pH buffering capacity (Bolan et al., 2003; Raut et al., 2012). The significant H^+-generating processes that occur during the biogeochemical cycling of C, N, and S can be accelerated by the activities of humans through intensive land-based crop and animal production, especially fertilization. Hence, in managed ecosystems used for agricultural production, regular fertilizer use is one of the major contributors to soil acidification. As a result, for instance in China, intensified agriculture since the early 1980s led to severe yield reductions and crop failures (Guo et al., 2010; Schroder et al., 2011; Zhou et al., 2014). Hence, one of the targets in this study was to investigate the effect of long-term fertilization (large inputs of chemical fertilizers and other resources) on soil pH since the early 1980s.

In addition to H^+ (activated acid), Al^{3+} (potential acid) is another important cation responsible for soil acidification. Al is present in multiple forms (e.g., Al^{3+}, $Al(OH)^{2+}$, $Al(OH)_2{}^+$, and polymeric Al) and is abundant in soils. During soil acidification, protons are initially consumed to release Al^{3+} from clay minerals, and the Al^{3+} is subject to hydrolysis to form Al-hydroxyl complexes or polymers, depending on the soil pH (Bolan et al., 2003). Moreover, the large buffering capacity of Al can result in high concentrations of toxic species from the continuous association with the produced protons. Many studies have focused on the regulation of aluminum toxicity, such as the interaction between Al-Ca (Kinraide, 1998), Al-Mg (Kinraide et al., 2004), Al-Si (Ma et al., 1997), Al-Mn (Blair and Taylor, 1997), and so on. However, those studies were mainly from the view of plant nutrition to illustrate the possible mechanisms of reducing Al toxicity to plants. Nevertheless, the changes in Al species accompanying soil acidification also need to be investigated.

From the view of geochemistry, aluminum and iron are the third and the fourth most abundant elements in the Earth's crust. In most intensively weathered soils of the tropics and subtropics (e.g., the Oxisols and Ultisols), goethite and hematite are the dominant Fe oxides. With the Al^{3+} ion (0.53 Å) being slightly smaller than the Fe^{3+} ion (0.65 Å), the ionic substitution of aluminum in iron oxides is well documented (Ekstrom et al., 2010; Li et al., 2016). Al substitution in iron oxides influences the crystal structure, unit cell parameters, crystallization rate, solubility surface properties, structural −OH content, magnetic hyperfine values and surface acidity of the minerals (de Carvalho Filho et al., 2015; Hu et al., 2014; Li et al., 2016; Pinney and Morgan, 2013). As a result, Al substitution in iron oxides can optimize the crystal structure of iron oxide and enhance its stability (Gonzalez et al., 2002; Liu et al., 2014; Pinney and Morgan, 2013). In contrast, the isomorphous substitution of Al for Fe in the structure also influences the activities of soil Al (da Costa et al., 2018; Sánchez-España et al., 2016a; Sánchez-España et al., 2016b). However, previous reports mainly focused on the interaction between Al and Fe as well as the effects of Al on the mineralogical properties of iron oxides. The deeper correlations among the isomorphous substitutions Al for Fe in the structure, soil Al activities, and soil acidification remain to be investigated. Hence, another target of this study was to investigate how different long-term fertilizer treatments influence the soil pH and chemical properties, especially the isomorphous substitution of Al for Fe and the constitution of the mineral phases in iron oxides.

In this study, a total of 66 topsoil (0 to 20 cm) samples from eleven long-term fertilization (LTF) treatments from 1990 to 2013 were collected from the Qiyang Red Soil Experimental Station in Hunan Province in subtropical China, a typical iron-rich red soil region. The iron oxides in the clay fraction of these samples were analyzed qualitatively and quantitatively and the ionic substitutions of Al for Fe in the structures of five typical treatments on clay samples in 2013 were calculated. The objective of this study was to investigate the influence of LTF on soil pH and its impact on the phase transformation of iron oxide minerals, especially on the mobilization of potential acid Al^{3+} in the soil during the transformation. This study will help us better understand soil acidification processes, and how those secondary minerals respond to soil pH during soil acidification.

2. Materials and methods

2.1. Site description and soil sampling

The research site is located at the Qiyang Red Soil Experimental Station of the Chinese Academy of Agricultural Science in Hunan Province in subtropical China (26°45′12″N, 111°52′32″E, 120 m altitude) (Cai et al., 2014). The area is characterized by a subtropical humid monsoon climate with hot, moist summers and cold, dry winters. The zonal soil is red soil developing from Quaternary Red Clay, and the soil is classified as Ferralic Cambisol (Wrb, 2006) with a clay texture. All eleven designated fertilization treatments were conducted on these sites that were established in the same upland field. Prior to the experiment, the topsoil (0 to 20 cm) was plowed before cultivation, and the field was under a high density of sorghum cultivation for three years (1988–1990) without any fertilization to ensure no apparent spatial difference in the soil physical and chemical properties in the plowing zone over the field. The basic characteristics of these research sites in 1990 were organic C (6.06 g/kg), N_{total} (1.07 g/kg), $N_{available}$ (0.79 g/kg), K_{total} (13.70 g/kg), $K_{available}$ (1.04 g/kg), P_{total} (0.45 g/kg), and $P_{available}$ (0.14 g/kg).

Eleven fertilization treatments have been applied since November 1990: (1) no fertilizer (Control); (2) chemical N fertilizer only (N); (3) chemical N and P fertilizers (NP); (4) chemical N and K fertilizers (NK); (5) chemical P and K fertilizers (PK); (6) chemical N, P, and K fertilizers (NPK); (7) chemical N, P, and K fertilizers with straw (NPKS); (8) chemical N, P, and K fertilizers plus manure (NPKM); (9) 1.5 times the chemical N, P, and K fertilizers plus manure (1.5NPKM); (10) chemical N, P, and K fertilizers plus manure with different planting patterns (NPKMR); and (11) only (M). The fertilizer applications of N, P_2O_5 and K_2O were 300 kg/hm^2, 120 kg/hm^2, and 120 kg/hm^2, respectively. The N, P and K minerals were urea (46% N), calcium superphosphate (12.5% P_2O_5) and potassium chloride (60.0% K_2O), respectively. The manure was pure pig manure with an average composition of 413.2 g/kg C and 16.7 g/kg N (on a dry weight basis) (Tong et al., 2014).

Each treatment was carried out on a 10 m × 9.8 m plot in a randomized block design and was replicated twice. Each plot was isolated by 100 cm cement baffle plates. These areas were cultivated with a maize (*Zea mays* L.)-wheat (*Triticum aestivium* L.) rotation, and no irrigation was given to either of the crops because the plots received high annual rainfall (mean = 1431 mm; n = 17) (Meng et al., 2014). Soil samples were collected from the topsoil (0 to 20 cm) in these 11 fertilization areas after the crops were harvested in October of 1990, 1997, 2002, 2007, 2011, and 2013, using a soil auger 5 cm in diameter. Crop residue on the soil surface was carefully removed before soil sampling. For each treatment, 10 soil samples were mixed into 1 composite soil sample in a random design. In total, 66 soil samples (6 × 11) were collected since 1990.

2.2. Analyses of soil physicochemical properties

The procedures for analyzing the major elements have been described elsewhere (Pansu and Gautheyrou, 2006; Tao et al., 2012). All measurements of the soil physicochemical properties, including the cation exchange capacity (CEC), soil pH, the exchangeable H^+ (H_{exch}) and exchangeable Al^{3+} (Al_{exch}), the amorphous (Fe_{Ox} and Al_{Ox}), free-state (Fe_{dith} and Al_{dith}), and organically bound (Fe_{py} and Al_{py}) iron and aluminum, were expressed from the air-dried soil equivalent. Specifically, the CEC of the soils was determined using the ammonium acetate method at pH 7.0 (Pansu and Gautheyrou, 2006). Soil pH was determined using a soil:water ratio of 1:1 and a pH meter with a combined

glass electrode. H_{exch} and Al_{exch} were determined using the potassium chloride exchange-neutralization titration method (Pollard et al., 1991). Fe_{Ox} and Al_{Ox} were extracted with an acidified ammonium oxalate buffer solution at pH 3.0 (Schwertmann, 1964). Fe_{dith} and Al_{dith} were extracted with a citrate-bicarbonate-dithionite (DCB) solution according to Mehra and Jackson (1958). Fe_{py} and Al_{py} were determined using alkaline sodium pyrophosphate at pH 8.5 (Alexandrova, 1960). The concentration of Fe in the extract was determined using the 1,10-phenanthroline method (Fadrus and Malý, 1975). The concentration of Al in the extract was determined by Inductive Coupled Plasma Emission Spectrometry (ICP).

2.3. Analyses of soil clay fraction

2.3.1. The preparation and fabrication of soil colloids

Among the 11 fertilization treatments, five typical treatments on soil samples in 2013 including the control, N, NPK, NPKM, and M were chosen and their clay sizes analyzed. Soil colloids were collected using natural sedimentation and the centrifugation method with modification (Gimbert et al., 2005). Specifically, the soil samples were air dried and sieved (2 mm). The experiments were conducted in a 200 mL beaker containing 20.00 g soil sample and 60 mL deionized water. The pH of the suspension was adjusted to 7–8 using 0.5 mol/L NaOH and was then ultrasonicated for 20 min with stirring. The soil suspension was then dispersed and sifted with a 320-mesh sieve into a beaker (keeping the total volume at 2000 mL). The clay fraction (< 2 μm) was extracted with a siphon, and the extracted colloidal suspension was flocculated with 0.5 mol/L $CaCl_2$. After removing the excess flocculating ions with deionized water and alcohol, the collected clay fraction was dried under an infrared lamp (50 °C). Following that, Fe_{Ox} and Fe_{dith}, Al_{Ox} and Al_{dith} in the collected clay fractions were directly measured using the same methods described above (Mehra and Jackson, 1958; Schwertmann, 1964).

2.3.2. Identification of the iron oxides by X-ray diffraction (XRD) analysis

The iron oxides in the clay fraction were identified using synchrotron X-ray diffraction (XRD) spectra. The collected soil colloids were divided into two groups, one was left untreated and the other was given a DCB treatment (Whittig and Allardice, 1986). The synchrotron XRD spectra were applied to collect these two types of colloid patterns, which were conducted with a Wiggler X-ray beamline source 17A1 (λ = 0.133367 nm, exposure time = 60 s, rotating rate = 300 rpm, scanning range = 2–60°) at the National Synchrotron Radiation Research Center in Hsinchu, Taiwan. The iron oxides were analyzed from the differential synchrotron X-ray diffraction (DXRD) signals between the untreated colloids and the DCB-treated colloids (Bigham et al., 2002). The relative content (%) of goethite and hematite in iron oxides can be calculated through their relative intensities of diagnostic diffraction peaks using Eqs. (1) and (2) (Liu et al., 1994; Schwertmann and Latham, 1986).

$$G\% = \frac{IntGoe(110)}{3.5 \times IntHem(012) + IntGoe(110)} \times 100\% \quad (1)$$

$$H\% = \frac{3.5 \times IntHem(012)}{3.5 \times IntHem(012) + IntGoe(110)} \times 100\% \quad (2)$$

where IntGoe(110) and IntHem(012) are the diffraction peak intensities of the goethite (110) and hematite (012) lines calculated by EVA Software, respectively.

2.3.3. Analysis of Al-substituted iron oxides

The Al substitution in iron oxides was calculated from the DXRD results. The values of the Al-substituted goethite ($G_{Al\ mol\%}$) and Al-substituted hematite ($H_{Al\ mol\%}$) were calculated through the shifts of their diagnostic diffraction peaks using Eqs. (3) and (4) (Liu et al., 1994; Schwertmann and Latham, 1986).

$$G_{Al\ mol\%} = 1730 - \frac{572}{\left(\frac{1}{d(111)^2} - \frac{1}{d(110)^2}\right)^{\frac{1}{2}}} \quad (3)$$

$$H_{Al\ mol\%} = 3109 - 617 \times 2d(110) \quad (4)$$

where Al mol% = [Al/(Al + Fe)] × 100%, d(111) and d(110) in Eq. (3) are the d (interplanar spacing) values of the goethite (111) and (110) line, respectively, and d(110) in Eq. (4) is the d value of the hematite (110) line.

Based on these test samples, the iron content of (Fe_{dith}-Fe_{Ox}) was wholly or mainly from the goethite and hematite. According to the amount of (Fe_{dith}-Fe_{Ox}), the G/H ratio (goethite/hematite) determined by XRD and the amount of Al substituted from crystalline iron oxides, the contents of goethite and hematite in the soil clay fraction could be calculated using Eqs. (5) to (8) (Liu et al., 1994; Schwertmann and Latham, 1986).

$$A = (x + y)/(x + y + m + n) \quad (5)$$

where A is the ratio of G/(G + H); x is the weight (g/kg of clay, the same below) of goethite; m is the weight of hematite; and y and n are the weights of Al substituted (i.e., AlOOH and Al_2O_3) in goethite and hematite (g/kg), respectively.

$$B = \left(\frac{y}{59.98}\right)/\left(\frac{y}{59.98} + \frac{x}{88.85}\right) \quad (6)$$

$$C = \left(\frac{n}{101.96}\right)/\left(\frac{n}{101.96} + \frac{m}{159.69}\right) \quad (7)$$

where B and C are the mol% Al of Al-substituted in goethite and hematite, respectively, 59.98 and 88.85 are the molecular weights of AlOOH and FeOOH, respectively, and 101.96 and 159.69 are the molecular weights of Al_2O_3 and Fe_2O_3, respectively.

$$D = x/1.591 + m/1.4297 \quad (8)$$

where D is the amount of Fe from crystalline iron oxides (Fe_{dith}-Fe_{Ox}) in the soil clay fraction (g/kg), which is assumed to be the total amount of Fe of goethite and hematite in the soil clay samples assuming that goethite and hematite are the predominant crystalline iron oxides in the red soils, 1.591 and 1.4297 are the transferring coefficients that change the weight of Fe into the weights of FeOOH and Fe_2O_3, respectively.

Finally, the four unknown parameters (x, y, m, and n) in the group of four linear equations (Eqs. (5) to (8)) could be calculated, and then the amount of iron oxides, aluminum in iron oxides, and the Al-substituted iron oxides ($IOs_{Almol\%}$) could be calculated using Eq. (9).

$$IOs_{Al\ mol\%} = \left(\frac{y}{59.98} + \frac{2n}{101.96}\right)/\left(\frac{y}{59.98} + \frac{2n}{101.96} + \frac{x}{88.85} + \frac{2m}{159.69}\right) \quad (9)$$

2.4. Statistical analysis

All statistical analyses of experimental data including the means of the soil CEC and the measured contents of Fe_{Ox}, Al_{Ox}, Fe_{dith}, Al_{dith}, Fe_{py}, Al_{py}, H_{exch} and Al_{exch} were performed using the SPSS 18.0 (SPSS, Inc., US) statistical software.

3. Results and discussion

3.1. Effects of long term fertilization on soil pH from 1990 to 2013

Fig. 1 shows a comparison of the soil acidification kinetics under these 11 fertilization systems from 1990 to 2013. From 1990 to 2013, the soil pH of the control treatment (no fertilizer) decreased from 5.70 to 5.62, and the yearly average acidification rate (ΔpH) was approximately $-0.003\ y^{-1}$ (Fig. 1). The soil pH under different types of LTF treatments presented significant differences. LTF using chemical

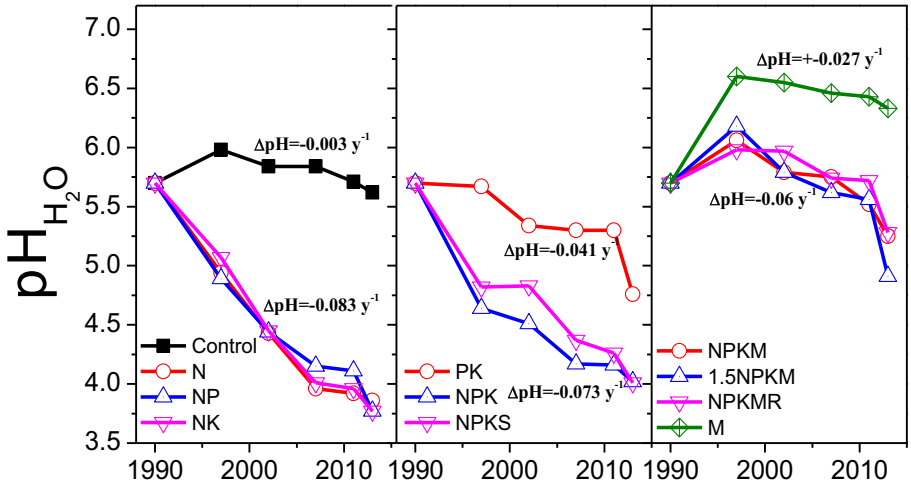

Fig. 1. Kinetics of soil pH under different fertilization systems from 1990 to 2013.

fertilizer containing N accelerated soil acidification. For instance, ΔpH under the N, NP and NK treatments was $-0.083\ y^{-1}$, whereas ΔpH under NPK and NPKS treatment was $-0.073\ y^{-1}$. Without N fertilizer, ΔpH under PK was $-0.041\ y^{-1}$. Compared with the above treatments, LTF using chemical fertilizer containing N plus M indicated that manure fertilizer could mitigate soil acidification. ΔpH under NPKM, 1.5NPKM, NPKMR treatment was $-0.024\ y^{-1}$, approximately one-third the ΔpH under the N, NP and NK treatments. Moreover, ΔpH under the M treatment was $+0.027\ y^{-1}$, indicating that M can increase the soil pH. Based on the kinetics of soil acidification, the rate of soil acidification increased in the following order: chemical fertilizer (N, NP, NK, NPK and NPKS) > PK > chemical with manure (NPKM, 1.5NPKM, NPKMR) > control > manure (M) (Fig. 1).

Furthermore, among the 11 different treatments, the calculated highest average soil pH value was 6.35 ± 0.41 (M fertilizer, n = 6), whereas the calculated lowest average soil pH value was 4.47 ± 0.73 (N fertilizer, n = 6) (Table 1). In a comparison of the calculated soil pH among the 11 different treatments, significant differences ($P < 0.01$) in the average soil pH values were observed between the control treatment (no fertilizer) and the chemical fertilizers (N, NP, NK, NPK and NPKS) (Table 1). Hence, as presented in Table 1 and Fig. 1, soil acidification rates were accelerated by chemical fertilizer, and a deacidification effect was observed with the manure fertilizer treatment.

3.2. Effects of long-term fertilization on soil aluminum from 1990 to 2013

Table 1 also presents the chemical properties of these soil samples under these 11 different long-term fertilization treatments. For instance, the average values of Al_{py} ranged from 0.08 ± 0.02 to 0.50 ± 0.20 g/kg (n = 6). The average values of Al_{exch} contents in the soils ranged from 0.16 ± 0.12 to 4.22 ± 2.40 g/kg (n = 6). Moreover, a comparison of these properties among the 11 different treatments revealed significant differences ($P < 0.01$) in the average values of Al_{py} between the control treatment and chemical fertilizers (N, NP, NK, NPK and NPKS) (Table 1). Similar trends were also observed in the average $Al_{exch.}$ values (Table 1). Nevertheless, anthropogenically induced soil acidification (i.e., chemical fertilizer treatments including N, NP, NK, NPK and NPKS) causes increased aluminum (Al_{py} and Al_{exch}) and hydrogen (H_{exch}) concentrations in soil solutions (Table 1). With the input of additional acidity in acidic soils, H^+ is initially consumed to release Al^{3+} from clay minerals, and Al^{3+} undergoes hydrolysis to form Al-hydroxyl complexes or polymers, depending on the soil pH (Bolan et al., 2003).

Furthermore, one target of this study was to investigate how different fertilizer treatments affect the pH and chemical properties of the soil; hence, a correlation analysis between soil pH and these chemical properties was conducted (Table 2). It showed that soil iron species (Fe_{dith}, Fe_{Ox}, and Fe_{py}) have weak correlations with soil pH, as indicated by the low Pearson's correlation coefficients of 0.06, 0.03 and 0.16, respectively. The correlations between soil aluminum species (Al_{dith}, Al_{Ox}, and Al_{py}), CEC, soil exchangeable acid (H_{exch} and Al_{exch}) and soil pH were significant at the 0.01 level, with Pearson's correlations of −0.44, −0.57, −0.88, 0.41, −0.60 and −0.87, respectively (Table 2). Moreover, Fig. 2 shows the scatter plots of measured soil pH values against the concentrations of soil aluminum species (Al_{Ox}, Al_{dith}, and Al_{py}), CEC, and soil exchangeable acid (H_{exch} and Al_{exch}). In general, scatter plots with R^2 values that approach unity indicate significant linear correlations. It was found that soil pH values only exhibited very strong negative linear correlations with values of $\log(Al_{py})$ ($R^2 = 0.76$) and $\log(Al_{exch})$ ($R^2 = 0.71$). In contrast, the correlations between soil pH and the values of $\log(Al_{Ox})$, $\log(H_{exch})$, $\log(Al_{dith})$ and log(CEC) were not significantly linearly correlated. The lower the soil pH values, the higher the concentrations of Al_{py} and Al_{exch} the soils possessed. These results further demonstrate that Al_{py} and Al_{exch} are more sensitive to soil acidification than the other factors.

On the other hand, as presented in Table 2 and Fig. 2, the total number of Al species ($Al_{dith} + Al_{Ox} + Al_{py}$) under different types of LTF indicated a negative correlation with pH, showing an increase in Al concentration with a decrease of soil pH under different conditions, especially for Al_{py} and Al_{exch}. In contrast, because of the strong selectivity of cation exchange sites for Al species, especially for Al^{3+}, Al saturation increases with decreasing pH (Baquy et al., 2018). The cations in the soil can coordinate with OH^- ions (the source of the water self-dissociation) (Sparks, 2018). Once OH^- is taken up by the cation, H^+ remains in the solution. Hence, soil acidification increases the active acid H^+ and the potential acid Al^{3+}, and an increase of Al^{3+} in the soil should be the most significant property accompanying soil acidification.

3.3. Effects of long-term fertilization on iron oxides in the clay fraction from 1990 to 2013

Synchrotron XRD spectra were applied to analyze the iron oxides in the clay fraction before and after the DCB treatments. The (111) and (110) lines of goethite, the (104), (110), (116) and (300) lines of hematite, the (120), (200) and (231) lines of lepidocrocite, and the (200), (400), and (511) lines of maghemite were scanned, and the subtracted diffraction pattern lines are presented in Fig. 3. Compared to the synchrotron XRD spectra before and after the DCB treatments (subtracting the background information), the differential X-ray diffraction pattern

Table 1
Properties of the soil samples on the basis of the air-dried soil mass from 1990 to 2013 (n = 6, the average value within the same column with different capital letters (i.e., A or B) are significantly different at $P < 0.01$, whereas average value within the same column with the same capital letters are not significantly different at $P = 0.01$.)

	pH	CEC[a]	Fe_{dith}[b]	Fe_{Ox}[b]	Fe_{py}[b]	Al_{dith}[b]	Al_{Ox}[b]	Al_{py}[b]	H_{exch}[c]	Al_{exch}[d]
Control	5.78 ± 0.13^{AB}	11.90 ± 0.56^{D}	39.23 ± 3.10^{ABCD}	2.53 ± 0.30^{ABC}	0.05 ± 0.01^{B}	3.81 ± 0.21^{B}	0.57 ± 0.05^{D}	0.14 ± 0.03^{DE}	0.07 ± 0.03^{C}	0.19 ± 0.11^{B}
N	4.47 ± 0.73^{D}	11.85 ± 0.57^{D}	35.16 ± 3.03^{CD}	2.36 ± 0.48^{BC}	0.07 ± 0.02^{AB}	4.12 ± 0.28^{AB}	0.85 ± 0.14^{A}	0.42 ± 0.17^{AB}	0.45 ± 0.20^{AB}	4.22 ± 2.40^{A}
NP	4.51 ± 0.69^{D}	12.58 ± 0.47^{CD}	38.06 ± 4.09^{BCD}	2.54 ± 0.62^{ABC}	0.07 ± 0.02^{AB}	4.18 ± 0.29^{AB}	0.82 ± 0.15^{A}	0.49 ± 0.24^{A}	0.43 ± 0.33^{AB}	3.56 ± 2.72^{A}
NK	4.49 ± 0.75^{D}	11.37 ± 0.76^{D}	40.08 ± 5.80^{ABC}	2.27 ± 0.30^{C}	0.07 ± 0.02^{AB}	4.11 ± 0.21^{AB}	0.70 ± 0.11^{ABCD}	0.43 ± 0.17^{AB}	0.59 ± 0.46^{A}	3.42 ± 2.40^{A}
PK	5.35 ± 0.34^{BC}	12.02 ± 0.61^{D}	45.38 ± 5.95^{A}	2.72 ± 0.40^{ABC}	0.06 ± 0.02^{AB}	4.17 ± 0.20^{AB}	0.63 ± 0.08^{BCD}	0.26 ± 0.15^{CD}	0.14 ± 0.09^{BC}	0.48 ± 0.48^{B}
NPK	4.53 ± 0.62^{D}	12.87 ± 0.90^{BCD}	42.00 ± 5.42^{AB}	2.71 ± 0.64^{ABC}	0.08 ± 0.02^{AB}	4.39 ± 0.25^{A}	0.79 ± 0.11^{AB}	0.50 ± 0.20^{A}	0.33 ± 0.16^{ABC}	3.66 ± 2.24^{A}
NPKM	5.68 ± 0.27^{AB}	14.08 ± 1.10^{AB}	37.95 ± 3.01^{BCD}	2.94 ± 0.64^{A}	0.09 ± 0.01^{AB}	3.98 ± 0.34^{AB}	0.75 ± 0.11^{ABCD}	0.28 ± 0.07^{BCD}	0.19 ± 0.06^{BC}	0.20 ± 0.17^{B}
1.5NPKM	5.63 ± 0.41^{ABC}	14.77 ± 1.22^{A}	38.77 ± 4.27^{BCD}	2.93 ± 0.70^{A}	0.12 ± 0.09^{A}	4.07 ± 0.14^{AB}	0.77 ± 0.19^{ABC}	0.34 ± 0.22^{ABC}	0.29 ± 0.19^{ABC}	0.21 ± 0.29^{B}
NPKS	4.88 ± 0.85^{CD}	12.02 ± 0.45^{D}	34.88 ± 3.98^{CD}	2.33 ± 0.36^{C}	0.08 ± 0.03^{AB}	3.99 ± 0.16^{AB}	0.77 ± 0.12^{AB}	0.45 ± 0.21^{A}	0.39 ± 0.21^{ABC}	3.09 ± 1.80^{A}
NPKMR	5.80 ± 0.37^{AB}	13.92 ± 1.50^{ABC}	32.78 ± 3.50^{D}	2.82 ± 0.72^{AB}	0.08 ± 0.03^{AB}	3.81 ± 0.32^{B}	0.72 ± 0.15^{ABCD}	0.25 ± 0.10^{CD}	0.19 ± 0.06^{BC}	0.16 ± 0.12^{B}
M	6.35 ± 0.41^{A}	14.54 ± 1.07^{AB}	41.22 ± 2.82^{ABC}	2.74 ± 0.24^{ABC}	0.10 ± 0.02^{AB}	3.81 ± 0.26^{B}	0.59 ± 0.03^{CD}	0.08 ± 0.02^{E}	0.15 ± 0.09^{BC}	0.20 ± 0.18^{B}

[a] cmol/kg (+).
[b] g/kg.
[c] cmol/kg(H^+).
[d] cmol/kg($1/3Al^{3+}$).

Table 2
Results of the correlation analysis between pH and chemical properties of the soil (n = 66).

		pH			pH
Fe_{dith}	P correlation	0.060	Al_{py}	P correlation	−0.878**
	Sig. (2-tailed)	0.625		Sig. (2-tailed)	0.000
Fe_{Ox}	P correlation	0.027	CEC	P correlation	0.409**
	Sig. (2-tailed)	0.830		Sig. (2-tailed)	0.000
Fe_{py}	P correlation	−0.157	$H_{exch.}$	P correlation	−0.604**
	Sig. (2-tailed)	0.200		Sig. (2-tailed)	0.000
Al_{dith}	P correlation	−0.436**	$Al_{exch.}$	P Correlation	−0.868**
	Sig. (2-tailed)	0.000		Sig. (2-tailed)	0.000
Al_{Ox}	P correlation	−0.573**			
	Sig. (2-tailed)	0.000			

** Correlation is significant at the 0.01 level (2-tailed).

(DXRD) revealed that goethite and hematite are the main types of iron oxides. The calculated results of G%, H%, and the G/H ratio are listed in Table 3. From Table 3, the calculated values of G% were in the range from 45% to 61%, and their corresponding G/H ratios were in the range from 0.8 to 1.6.

Compared with the G/H value (0.95) and the amount of goethite (x, 22.22 g/kg) of the control in 2013, the results obtained reveal the different impacts of LTF treatments on iron oxides in the clay fractions. Specifically, LTF treatment with chemical N reduced the G/H value (0.84). The decreased amount of goethite (x, 19.4 g/kg), as well as the decreased percentage of goethite in the total iron oxides (45.79%), in the N treatment may reflect the hydrolyzation and recrystallization of Fe^{3+} in soil solutions, which would further illustrate the aging courses of iron oxides during the LTF treatment. In contrast, the LTF treatments with manure (NPKM and M) increased the G/H values (1.51 and 1.46) above the check samples, and the increased amount of goethite (28.17 and 25.91 g/kg) as well as the increased percentage of goethite in the total iron oxides (60.12% and 59.35%)s may be attributed to the dissimilar dissolution of iron oxides under the effects of organic matter. The dissimilar dissolution rates of iron oxides in the soil would be accelerated under the effects of organic matter (attributed to the complex effects and the electron shuttle effect), and the freshly generated Fe(II) would further recrystallize to various iron oxides, i.e., ferrihydrite, goethite, hematite, and so on (Zhu et al., 2014).

On the other hand, compared with the content of hematite (m, 25.65 g/kg) in the control in 2013, the hematite content in the other check samples were decreased (Table 3). Nevertheless, compared with the percentage of hematite (51.25%) of the control in 2013, the other checked samples presented different characteristics. Specifically, the LTF treatment with chemical N increased the percentage of hematite (54.21%), whereas the other three treatments reduced those values (47.56%, 39.88% and 40.56%). By applying the one site-two pKa SCMs (surface complexation models), previous studies (Cheng et al., 2017; Wang et al., 2018) have evaluated the acid-base properties of soils, and the results have proved that the accumulation of hematite (%) in soils would decrease the total amount of active sites in soil surface, which would further reduce the mitigation abilities of the soil to acidification.

3.4. Effects of long-term fertilization on the isomorphous substitution of Al for Fe in iron oxides from 1990 to 2013

Table 3 also shows that Al substitution in goethite and hematite was in the range of 9% to 24%, and the $G_{Al\ mol\%}$ and $H_{Al\ mol\%}$ in the control were 23.30 mol% and 13.22 mol%, respectively. Moreover, as shown in Table 3, the calculated contents of iron oxides (x + m) ranged from 41.00 to 50.00 g/kg, the weight of Al-substituted (AlOOH and Al_2O_3) in iron oxides (y + n) ranged from 4.00 to 7.30 g/kg, and the calculated results of $IOs_{Almol\%}$ ranged from 13.00 to 20.00 mol%. Furthermore, the soil pH under different LTF systems increased in the order of N (3.86) < NPK (4.02) < NPKM (5.25) < Control (5.62) < M (6.33),

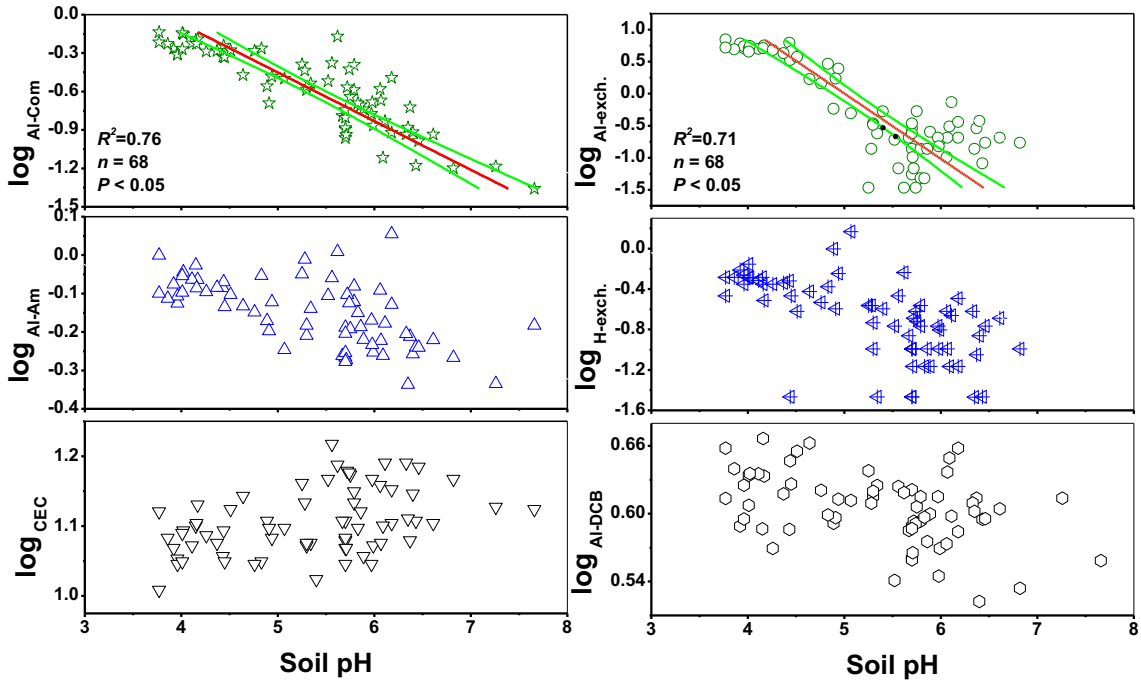

Fig. 2. Scatter plots of the concentrations of soil aluminum species (Al_{Ox}, Al_{dith}, and Al_{py}), CEC, and soil exchangeable acid (H_{exch} and Al_{exch}) against measured soil pH values.

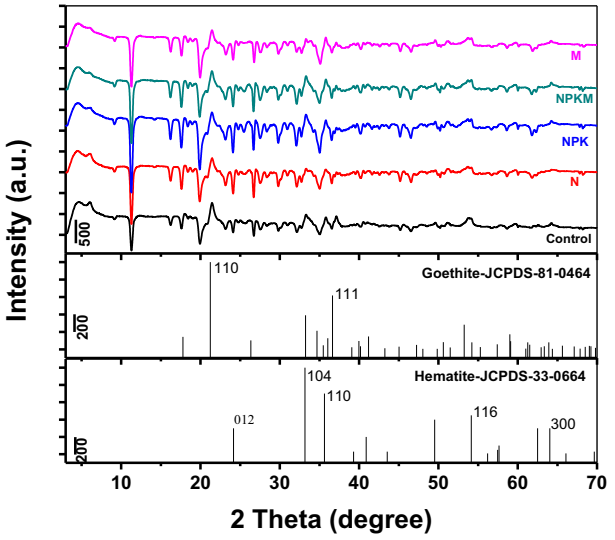

Fig. 3. Differential X-ray diffraction pattern (DXRD) results of iron oxides in clay minerals.

and the values of $IOs_{Almol\%}$ also experienced the following increasing trend: N (13.44 mol%) < NPK (16.05 mol%) < NPKM (16.20 mol %) < Control (17.96 mol%) < M (19.17 mol%).

On the other hand, soil pH is mainly determined by two factors, the activated acid H^+ and the potential acid Al^{3+}. As Al is present in multiple forms and is abundant in soils, especially in tropical/subtropical soils, trying to reduce the activity of the potential acid Al^{3+} in the soil should be a feasible way to mitigate soil acidification. Fig. 4 presents the relationship between the soil pH and its corresponding $IOs_{Almol\%}$ in 2013 under different LTF systems. A positive relationship exists between soil pH and its corresponding $IOs_{Almol\%}$ under these typical different LTF systems. The higher the soil pH, the higher is the $IOs_{Almol\%}$ (Fig. 4). Hence, the isomorphous substitution of Al for Fe in iron oxides could possibility decrease the dissolution of Al^{3+} ions and reduce the concentration and the mobilization of potential acid Al^{3+} in the soil. Furthermore, the decreased mobilization of potential acid Al^{3+} in soil would further mitigate soil acidification. To prove this hypothesis, however, further studies are needed to investigate the possible mechanisms.

4. Conclusions

Following 23 years (1990–2013) of LTF on maize and wheat

Table 3
Contents of iron oxide in the clay fraction and Al substitution in iron oxides in 2013.

	pH	Fe_{dith}-Fe_{Ox} (g/kg)	Al_{dith}-Al_{Ox}(g/kg)	Goethite (%)	Hematite (%)	G/H ratio	Al in goethite (mol%)	Al in hematite (mol%)	x (g/kg)	y (g/kg)	m (g/kg)	n (g/kg)	IOs_{Al} (mol%)
Control	5.62	31.91	3.33	48.75	51.25	0.95	23.30	13.22	22.22	4.56	25.65	2.50	17.96
N	3.86	27.44	3.59	45.79	54.21	0.84	9.28	16.49	19.40	1.34	21.80	2.75	13.44
NPK	4.02	32.69	3.42	52.44	47.56	1.10	11.64	21.40	26.86	2.09	22.60	3.93	16.05
NPKM	5.25	31.33	3.46	60.12	39.88	1.51	18.03	13.75	28.17	4.18	19.48	1.98	16.21
M	6.33	29.68	3.36	59.35	40.65	1.46	22.57	14.62	25.91	5.10	19.15	2.09	19.17

x: weights of goethite.
y: weights of Al substituted (AlOOH) in goethite.
m: weights of hematite.
n: weights of Al substituted (Al_2O_3) in hematite.

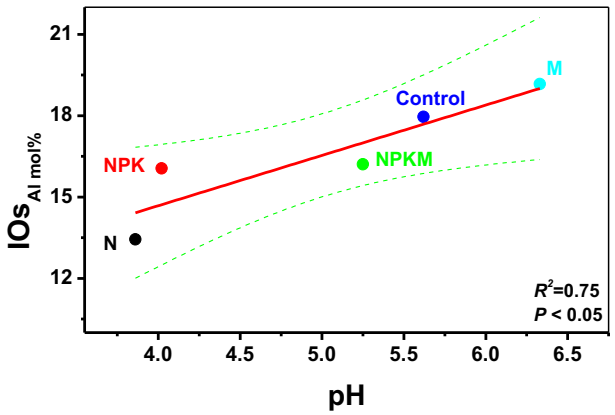

Fig. 4. Correlation between the soil pH and its corresponding Al substitution in iron oxides ($IOs_{Almol\%}$).

rotation cropping, chemical fertilizer accelerated and manure fertilizer decelerated soil acidification, whereas the soil pH was closely correlated with two critical aluminum species ($log(Al_{py})$ and $log(Al_{exch})$) in a negative linear relationship, and an increase in Al^{3+} in soil should be the most significant property accompanying soil acidification. Furthermore, the LTF treatment with chemical N reduced the total content of iron oxides and the G/H value, whereas the LTF treatments with manure (NPKM and M) exhibited the opposite trends. The transformation of iron oxides (i.e., goethite to hematite) as well as the accumulation of hematite in the soil would reduce the abilities of the soil to mitigate acidification. Moreover, a positive relationship proved to exist between the soil pH and its corresponding $IOs_{Almol\%}$. This study presents a novel view on recognizing how possible soil acidification or deacidification occurs during LTF, and the mineralogical response of the iron oxides to the change in soil pH induced by LTF. However, further studies are required to reveal the contribution and exact mechanism of iron oxides on the mitigation of soil acidification.

Acknowledgments

The authors thank Professor Dean Hesterberg at the department of Crop and Soil Science, North Carolina State University, United States for his valuable comments on the manuscript during its preparation. This work was financially supported by the National Key Basic Research Program of China (Nos. 2014CB441002 and 2014CB441001), the National Natural Science Foundation of China (No. 41877038), Guangdong Natural Science Foundation for Distinguished Young Scholars (No. 2016A030306019), the Natural Science Foundation of Guangdong Province (No. 2018A030313385), GDAS' Project of Science and Technology Development (No. 2017GDASCX-0407), and the Local Innovative and Research Teams Project of Guangdong Pearl River Talents Program (No. 2017BT01Z176). The synchrotron XRD experiments were carried out at the National Synchrotron Radiation Research Center in Hsinchu, Taiwan.

References

Alexandrova, L.N., 1960. On the composition of humus substances and the nature of órgano-mineral colloids in soil. In: Transactions Int. Congr. Soil Sci, pp. 74–81.
Baquy, M.A.A., Li, J.Y., Jiang, J., Mehmood, K., Shi, R.Y., Xu, R.K., 2018. Critical pH and exchangeable Al of four acidic soils derived from different parent materials for maize crops. J. Soils Sediments 18, 1490–1499.
Bigham, J.M., Fitzpatrick, R.W., Schulze, D.G., 2002. Iron oxides. In: Dixon, J.B., Schulze, D.G. (Eds.), Soil Mineralogy With Environmental Applications. Soil Science Society of America, Madison, WI, pp. 323–366.
Blair, L.M., Taylor, G.J., 1997. The nature of interaction between aluminum and manganese on growth and metal accumulation in *Triticum aestivum*. Environ. Exp. Bot. 37, 25–37.
Blake, L., Johnston, A.E., Goulding, K.W.T., 1994. Mobilization of aluminium in soil by acid deposition and its uptake by grass cut for hay – a chemical time bomb. Soil Use Manag. 10, 51–55.
Bolan, N.S., Adriano, D.C., Curtin, D., 2003. Soil acidification and liming interactions with nutrient and heavy metal transformation and bioavailability. Adv. Agron. 78, 215–272.
Breemen, N.V., 1991. Soil Acidification and Alkalinization. Springer Berlin Heidelberg.
Bünemann, E.K., Bongiorno, G., Bai, Z.G., Creamer, R.E., De Deyn, G., de Goede, R., Fleskens, L., Geissen, V., Kuyper, T.W., Mäder, P., Pulleman, M., Sukkel, W., van Groenigen, J.W., Brussaard, L., 2018. Soil quality – a critical review. Soil Biol. Biochem. 120, 105–125.
Cai, Z.J., Wang, B.R., Xu, M.G., Zhang, H.M., He, X.H., Zhang, L., Gao, S.D., 2014. Intensified soil acidification from chemical N fertilization and prevention by manure in an 18-year field experiment in the red soil of southern China. J. Soils Sediments 15, 260–270.
de Carvalho Filho, A., Inda, A.V., Fink, J.R., Curi, N., 2015. Iron oxides in soils of different lithological origins in Ferriferous Quadrilateral (Minas Gerais, Brazil). Appl. Clay Sci. 118, 1–7.
Cheng, P.F., Wang, Y., Cheng, K., Li, F.B., Chen, H.L., Liu, T.X., 2017. The acid-base buffer capacity of red soil variable charge minerals and its surface complexation model. Acta Chim. Sin. 75, 637–644 (Chinese Edition).
da Costa, E.U.C., dos Santos, J.C.B., de Azevedo, A.C., de Araújo, F., José, C.C., Marcelo, M., de Melo, W.N., Laércio, V., Vidal-Torrado, P., Souza-Júnior, V.S., 2018. Mineral alteration and genesis of Al–rich soils derived from conglomerate deposits in Cabo Basin, NE Brazil. Catena 167, 198–211.
Ekstrom, E.B., Learman, D.R., Madden, A.S., Hansel, C.M., 2010. Contrasting effects of Al substitution on microbial reduction of Fe(III) (hydr)oxides. Geochim. Cosmochim. Acta 74, 7086–7099.
Fadrus, H., Malý, J., 1975. Rapid extraction-photometric determination of traces of iron (II) and iron(III) in water with 1,10-phenanthroline. Anal. Chim. Acta 77, 315–316.
Gimbert, L.J., Haygarth, P.M., Ronald, B., Worsfold, P.J., 2005. Comparison of centrifugation and filtration techniques for the size fractionation of colloidal material in soil suspensions using sedimentation field-flow fractionation. J. Neurophysiol. 39, 1731–1735.
Gonzalez, E., Ballesteros, M.C., Rueda, E.H., 2002. Reductive dissolution kinetics of Al-substituted goethites. Clay Clay Miner. 50, 470–477.
Guo, J.H., Liu, X.J., Zhang, Y., Shen, J.L., Han, W.X., Zhang, W.F., Christie, P., Goulding, K.W., Vitousek, P.M., Zhang, F.S., 2010. Significant acidification in major Chinese croplands. Science 327, 1008–1010.
Hu, Y., Li, Q., Lee, B., Jun, Y.S., 2014. Aluminum affects heterogeneous Fe(III) (Hydr) oxide nucleation, growth, and ostwald ripening. Environ. Sci. Technol. 48, 299–306.
Kinraide, T.B., 1998. Three mechanisms for the calcium alleviation of mineral toxicities. Plant Physiol. 118, 513–520.
Kinraide, T.B., Pedler, J.F., Parker, D.R., 2004. Relative effectiveness of calcium and magnesium in the alleviation of rhizotoxicity in wheat induced by copper, zinc, aluminum, sodium, and low pH. Plant Soil 259, 201–208.
Li, W., Wang, L.J., Liu, F., Liang, X.L., Feng, X.H., Tan, W.F., Zheng, L.R., Yin, H., 2016. Effects of Al^{3+} doping on the structure and properties of goethite and its adsorption behavior towards phosphate. J. Environ. Sci. 45, 18–27.
Liu, F., Xu, F.L., Li, X.Y., Wang, Y.J., Zeng, G.Q., 1994. Types of crystalline iron oxides and phosphate adsorption in variable charge soils. Pedosphere 4, 35–46.
Liu, T.X., Li, X.M., Li, F.B., Tao, L., Liu, H., 2014. Effects of Al content and synthesis temperature on Al-substituted Fe oxides. Soil Sci. 179, 468–475.
Ma, J.F., Sasaki, M., Matsumoto, H., 1997. Al-induced inhibition of root elongation in corn, *Zea mays* L. is overcome by Si addition. Plant Soil 188, 171–176.
Mehra, O.P., Jackson, M.L., 1958. Iron oxide removed from soils and clays by a dithionite-citrate system buffered with sodium bicarbonate. Clay Clay Miner. 7, 317–329.
Meng, H.Q., Xu, M.G., Lv, J.L., He, X.H., Wang, B.R., Cai, Z.J., 2014. Quantification of anthropogenic acidification under long-term fertilization in the upland red soil of South China. Soil Sci. 179, 486–494.
Pansu, M., Gautheyrou, J., 2006. Handbook of Soil Analysis: Mineralogical, Organic and Inorganic Methods. Springer, Netherlands.
Pinney, N., Morgan, D., 2013. Thermodynamics of Al-substitution in Fe-oxyhydroxides. Geochim. Cosmochim. Acta 120, 514–530.
Pollard, R.J., Pankhurst, Q.A., Zientek, P., 1991. Magnetism in aluminous goethite. Phys. Chem. Miner. 18, 259–264.
Raut, N., Dörsch, P., Sitaula, B.K., Bakken, L.R., 2012. Soil acidification by intensified crop production in South Asia results in higher N2O/(N2 + N2O) product ratios of denitrification. Soil Biol. Biochem. 55, 104–112.
Rice, K.C., Herman, J.S., 2012. Acidification of Earth: an assessment across mechanisms and scales. Appl. Geochem. 27, 1–14.
Sánchez-España, J., Yusta, I., Burgos, W.D., 2016a. Geochemistry of dissolved aluminum at low pH: hydrobasaluminite formation and interaction with trace metals, silica and microbial cells under anoxic conditions. Chem. Geol. 441, 124–137.
Sánchez-España, J., Yusta, I., Gray, J., Burgos, W.D., 2016b. Geochemistry of dissolved aluminum at low pH: extent and significance of Al–Fe(III) coprecipitation below pH 4.0. Geochim. Cosmochim. Acta 175, 128–149.
Schroder, J.L., Zhang, H.L., Girma, K., Raun, W.R., Penn, C.J., Payton, M.E., 2011. Soil acidification from long-term use of nitrogen fertilizers on winter wheat. Soil Sci. Soc. Am. J. 75, 957–964.
Schwertmann, U., 1964. Differenzierung der eisenoxide des bodens durch photochemische extraktion mit sauer ammoniumoxalat-losung. Z. Pflanzenernähr. Bodenkd. 105, 194–202.
Schwertmann, U., Latham, M., 1986. Properties of iron oxides in some new caledonian oxisols. Geoderma 39, 105–123.
Sparks, D.L. (Ed.), 2018. Soil Physical Chemistry, Second edition. CRC Press, Boca Raton.
Speir, T.W., Kettles, H.A., Percival, H.J., Parshotam, A., 1999. Is soil acidification the cause of biochemical responses when soils are amended with heavy metal salts. Soil

Biol. Biochem. 31, 1953–1961.
Tao, L., Zhang, W., Li, H., Li, F.B., Yu, W.M., Chen, M.J., 2012. Effect of pH and weathering indices on the reductive transformation of 2-nitrophenol in South China. Soil Sci. Soc. Am. J. 76, 1579–1591.
Tong, X.G., Xu, M.G., Wang, X.J., Bhattacharyya, R.J., Zhang, W.J., Cong, R.H., 2014. Long-term fertilization effects on organic carbon fractions in a red soil of China. Catena 113, 251–259.
Wang, Y., Cheng, P.F., Li, F.B., Liu, T.X., Cheng, K., Yang, J.L., Lu, Y., 2018. Variable charges of a red soil from different depths: acid-base buffer capacity and surface complexation model. Appl. Clay Sci. 159, 107–115.
Whittig, L.D., Allardice, W.R., 1986. X-ray diffraction techniques. In: Agronomy. A Series of Monographs - American Society of Agronomy.
Wrb, 2006. I.W.G. World reference base for soil resources 2006: a framework for international classification, correlation and communication. FAO, Rome (World Soil Resources Reports 103) - ISBN 9251055114 - p.
Zhou, J., Xia, F., Liu, X.M., He, Y., Xu, J.M., Brookes, P.C., 2014. Effects of nitrogen fertilizer on the acidification of two typical acid soils in South China. J. Soils Sediments 14, 415–422.
Zhu, Z.K., Tao, L., Li, F.B., 2014. 2-Nitrophenol reduction promoted by S. putrefaciens 200 and biogenic ferrous iron: the role of different size-fractions of dissolved organic matter. J. Hazard. Mater. 279, 436–443.